Asymmetric nonlinear response of the quantized Hall effect

2010 New J. Phys. 12 113011

(http://iopscience.iop.org/1367-2630/12/11/113011)

New Journal of Physics
The open-access journal for physics

Asymmetric nonlinear response of the quantized Hall effect

A Siddiki[1,2,4,5], **J Horas**[1], **D Kupidura**[1], **W Wegscheider**[3] **and S Ludwig**[1]

[1] Center for NanoScience and Fakultät für Physik, Ludwig-Maximilians-Universität, Geschwister-Scholl-Platz 1, D-80539 München, Germany
[2] Physics Department, Faculty of Arts and Sciences, Istanbul University, 34134 Vezneciler, Istanbul, Turkey
[3] Laboratory for Solid State Physics, ETH Zürich, CH-8093 Zürich, Switzerland
E-mail: asiddiki@fas.harvard.edu

New Journal of Physics **12** (2010) 113011 (10pp)
Received 9 July 2010
Published 8 November 2010
Online at http://www.njp.org/
doi:10.1088/1367-2630/12/11/113011

Abstract. An asymmetric breakdown of the integer quantized Hall effect (IQHE) is investigated. This rectification effect is observed as a function of the current value and its direction in conjunction with an asymmetric lateral confinement potential defining the Hall bar. Our electrostatic definition of the Hall bar via Schottky gates allows a systematic control of the steepness of the confinement potential at the edges of the Hall bar. A softer edge (flatter confinement potential) results in more stable Hall plateaus, i.e. a breakdown at a larger current density. For one soft and one hard edge, the breakdown current depends on its direction, resembling rectification. This nonlinear magneto-transport effect confirms the predictions of an emerging screening theory of the IQHE.

[4] Current address: Physics Department, Harvard University, Cambridge, 02138 MA, USA.
[5] Author to whom any correspondence should be addressed.

Contents

1. Introduction

The discovery of the integer quantized Hall effect (IQHE) [1] in a two-dimensional electron system (2DES) subjected to a perpendicular magnetic field B opened up a wide research field in solid state physics, which has become a paradigm since then [2]. In spite of many experimental [3–6] and theoretical [7–10] efforts, our understanding of the IQHE is still far from being complete. The conventional theories [7, 9, 11] can successfully describe the main features of the IQHE, namely the existence of extended Hall plateaus and their extremely accurate quantized resistance values. Relying on a single-particle picture, they fail to give a comprehensive description of many experimental observations on a more detailed level. These original edge or bulk theories disregard the classical Hartree-type (direct) Coulomb interaction within the 2DES altogether [7–9]. The bulk theories assume the current to flow through the entire Hall bar [11]. On the basis of wafer properties such as disorder, they predict localized states. The edge theories describe the Hall plateaus by assuming current flow only along the edges of the Hall bar [9]. However, an explanation of the transition region between plateaus requires the additional assumption of localized bulk states caused by disorder similar to that of the bulk theories. Since these conventional theories rely on disorder, one could come to a conclusion that no QHE would occur in a hypothetical perfect sample free of disorder. This is proven to be incomplete by a newer approach that disregards disorder but includes the direct Coulomb interaction between electrons moving in the confinement potential in a self-consistent manner [12]. Building on this model, a comprehensive screening theory emerged. It self-consistently takes into account the Coulomb interaction and also considers disorder as well as the quantum mechanical wavefunctions of the electrons [13, 14]. For the Fermi energy approximately centered in between the energies of two adjacent Landau levels, the screening theory predicts that the current is carried by incompressible regions (strips) extending along the Hall bar, hence replacing the edge channels. Since back scattering is absent within an incompressible region, this explains the observation of the Hall plateaus. Because our self-consistent approach takes into account the exact shape of the confinement potential and, in addition, can explicitly consider the nonlinear transport [15, 16], it allows for predictions that are beyond the scope of the conventional theories. Effects based on the electron spin such as exchange interaction are not taken into account here, but can be included [17–20].

A prominent non-equilibrium phenomenon observed at quantized Hall systems is the electrical breakdown [21–24], where the IQHE disappears as the current flowing through the Hall bar exceeds its breakdown value. It is usually attributed to a non-equilibrium occupation of the higher Landau levels and has been discussed within the above-mentioned non-interacting single-particle models. In the past, it has already been observed that the breakdown of the

IQHE is correlated with the asymmetries of the confinement potential of the Hall bar [25]. More recently, the effect of sample mobility together with sample width have been investigated experimentally and two distinct breakdown regimes have been reported [26]. In addition, an impurity-assisted inter-Landau-level tunneling mechanism has been proposed by Guven *et al* [27], to explain the observed excitation time scales [28].

In this work, we present nonlinear magneto-transport measurements and discuss them within the framework of the screening theory. We experimentally investigate the current-induced breakdown of the IQHE in narrow gate-defined Hall bars with confinement potentials that are asymmetric in the lateral direction. In detail, we demonstrate a situation in which dissipation-suppressed current only exists in one of the two current directions along the Hall bar. This rectification of the IQHE occurs in a wide range of parameters such as the mobility, charge carrier density and Hall bar width. The screening theory predicts the observed behavior for our high-mobility Hall bars assuming that the long-range potential fluctuations due to disorder do not destroy the formation of the incompressible strips at the edges [14].

2. Experimental setup and sample properties

Our Hall bars are electrostatically defined by means of metallic Schottky gates produced by electron-beam lithography on the surfaces of high-mobility AlGaAs/GaAs heterostructures containing 2DESs 110 nm beneath the surface. This field-effect method allows us to define Hall bars with extremely smooth and selectively tunable confinement potentials. A typical gate layout is displayed in the SEM picture of figure 1(a). A constant dc current is impressed between the source (S) and drain (D) contacts, while four more ohmic contacts A_1, A_2 and B_1, B_2 are used as voltage probes. The Hall resistance R_H is obtained by measuring the voltage drop between contacts A_1 and B_1 or A_2 and B_2, while the longitudinal resistance R_L is measured with A_1 and A_2 or B_1 and B_2. For simplicity, we will not specify which of these combinations of contacts are used in the following, given that our measurements are roughly independent of it. In order to create a laterally asymmetric confinement potential, we apply different gate voltages V_L and V_R along the two sides of the Hall bar, while the three gates on each side are always on equal potential. In all measurements shown here, B is perpendicular to the 2DES and points upwards, thus defining left-handed chirality, as sketched in figure 1(a) for the linear response case (dashed arrows indicate the direction that electrons move in equilibrium). $I_{SD} > 0$ corresponds to $V_S > 0$, while the drain contact is always grounded $V_D = 0$ (for the measurements shown in this paper). Figures 1(b)–(d) sketch the energy of the relevant Landau level (thin dashed line) for $I_{SD} = 0$ (figure 1(a)), $I_{SD} > 0$ (figure 1(b)) and $I_{SD} < 0$ (figure 1(c)) as predicted by the screening theory for the Hall plateaus [14]. The relevant Landau level is the one that is pinned to the chemical potentials at the edges of the Hall bar. Also shown is the electro-chemical potential $\mu^*(x)$ (thick dashed line) across the Hall bar, which includes the effect of a non-zero current, i.e. the non-equilibrium case. The shaded areas mark the width of incompressible regions and will be discussed below. We have performed measurements on five different samples with a Hall bar width of 3 μm or 10 μm and mobilities of $\mu \simeq 1.4 \times 10^6\,\mathrm{cm^2\,Vs^{-1}}$, $\mu \simeq 3 \times 10^6\,\mathrm{cm^2\,Vs^{-1}}$ and $\mu \simeq 8 \times 10^6\,\mathrm{cm^2\,Vs^{-1}}$ on wafers I, II and III, respectively. Here, we only present data measured on wafers I and III at a temperature of $T \simeq 1.7$ K. However, many more data taken so far confirm the results discussed below. It is important to note that the voltages applied to the confining gates are more negative than the pinch-off bias measured to be ~ -0.25 V. This is experimentally tested and implies that the side gates are wide enough to prevent any leakage currents across the

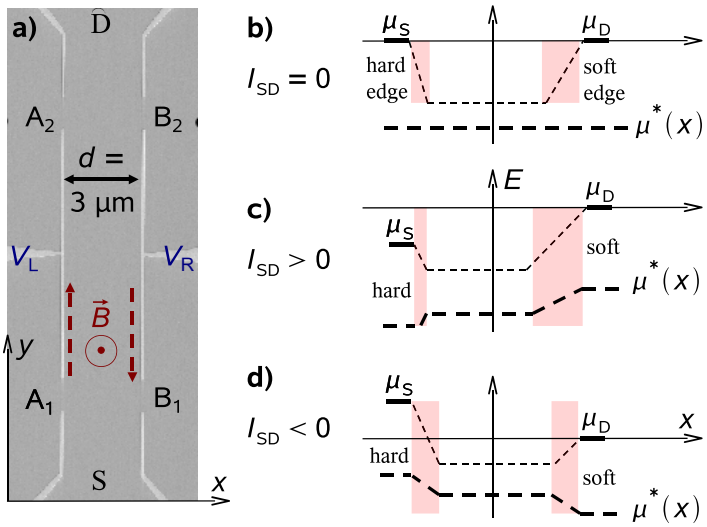

Figure 1. (a) Scanning electron microscope photograph of a typical sample. Top gates are colored in light gray. The voltage V_L (V_R) is applied to the three lhs (rhs) gates. A constant current I_{SD} is impressed at the source (S) contact and flows into the grounded drain (D) contact. The other ohmic contacts A_1, A_2, B_1 and B_2 are used as voltage probes. A magnetic field perpendicular to the 2DES is directed upward and defines a left-handed chirality for electrons moving along the 2DES (dashed arrows), which are essentially the (Landauer–Büttiker) edge state electrons. (b) Qualitative sketch of the energy of the relevant Landau level (thin dashed line), which is pinned to the chemical potential (Fermi energy) at the edges. Here $I_{SD} = 0$ and $V_L < V_R < V_{depl} < 0$, where at V_{depl} the 2DES beneath a gate is completely depleted; μ_S and μ_D are the chemical potentials defined at the source versus drain contacts. Also shown is the electro-chemical potential $\mu^*(x)$ (thick dashed line) across the Hall bar. The shaded areas mark the width of incompressible regions. (c, d) The same as (b) but for the non-equilibrium case $I_{SD} > 0$ or $I_{SD} < 0$.

electrostatically defined barriers to the side contacts A_1, A_2, B_1 and B_2. In the pinch-off regime, we can indeed assume that the width of the barriers exceeds the width of the confining gates of 100 nm, which is at least an order of magnitude larger than the magnetic length—the relevant length scale that defines the overlap of the electronic wavefunctions. Hence, we can neglect leakage currents caused by tunneling of electrons below the side gates.

3. Results and discussion

It has often been argued that applying a higher gate voltage should result in a softer edge potential profile (as e.g. proposed in [10]). However, numerical results obtained by solving the 3D Poisson equation self-consistently indicate just the opposite: for a more negative gate voltage applied, the density profile becomes sharper [29]. Our own numerical results are shown in figure 2, where an efficient fourth-order grid technique is used to obtain electrostatic quantities for the specific wafer parameters and applied gate voltages. Clearly, the steepness of

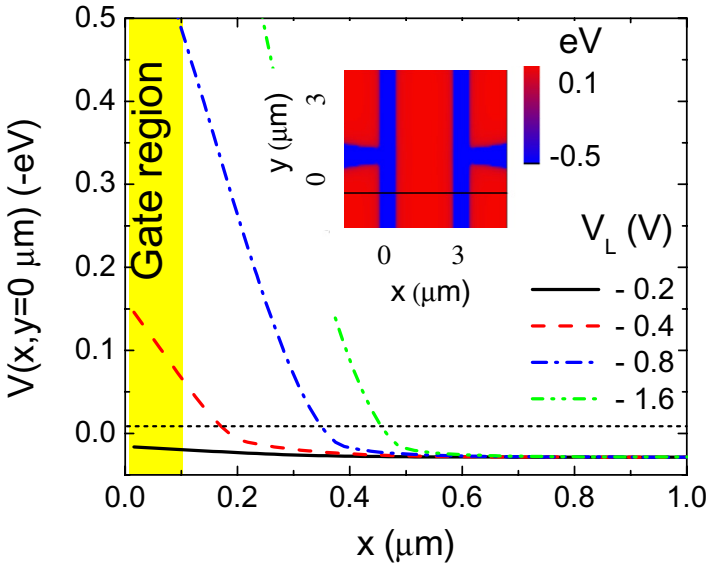

Figure 2. Self-consistently calculated electrostatic potentials as a function of the distance to the gates shown for four representative negative gate voltages. The horizontal dashed line indicates the Fermi energy $E_F \simeq 10.75$ meV. The shaded area (yellow) indicates the gated region. Directly below the gates the 2DES is depleted for gate voltages below -0.25 V (pinch-off regime). The inset shows the calculated potential distribution in 2D for the symmetric case of $V_L = V_R = -1.5$ V applied to the gates on both sides of the Hall bar. Data shown in the main figure are calculated along the horizontal line in the inset. Note that all the dark (blue) regions are depleted at the inset.

the confinement potential increases strongly as the gate voltage is decreased (to more negative values). We find that the depletion length increase is weaker than proportional to the applied gate voltage, other than previously predicted in [10].

Figure 3 displays the measured Hall resistance R_H of a Hall bar realized in wafer I ($d = 10\,\mu$m) as a function of the perpendicular magnetic field $0 < B < 3.5$ T. The gate voltages are $V_L = -1.2$ V and $V_R = -0.3$ V. They create a harder confinement potential on the left-hand side (lhs) of the Hall bar compared to the relatively soft rhs edge (see figure 1(b)). The Hall curves displayed in figure 3 are measured at $I_{SD} = \mp 2\,\mu$A (lhs y-axis) and $I_{SD} = \mp 5\,\mu$A (rhs y-axis). Parts of the curves, namely in the region of filling factors $\nu \simeq 6$ and $\nu \simeq 4$, are shown again in the inset of figure 3, where we have also added data for $I_{SD} = \mp 10\,\mu$A (curves for $I_{SD} = \mp 5\,\mu$A and $I_{SD} = \mp 10\,\mu$A are vertically shifted). For $I_{SD} = \mp 2\,\mu$A, the Hall plateaus are well established, where they are pretty much smeared out for $I_{SD} = \mp 10\,\mu$A, independent of the current direction. This observation can be attributed to the well-known breakdown of the IQHE, usually explained (within the edge channel models) by scattering between (many) edge channels [27]. Interestingly, for the intermediate current value of $I_{SD} = \mp 5\,\mu$A, the breakdown is more pronounced for one of the two current directions, namely $I_{SD} < 0$.

Exactly this behavior is predicted by the screening theory [14]; within this calculation scheme the current-induced breakdown of the IQHE is caused by inelastic scattering between compressible regions (Joule heating) [30]. Essentially the width of the incompressible strips

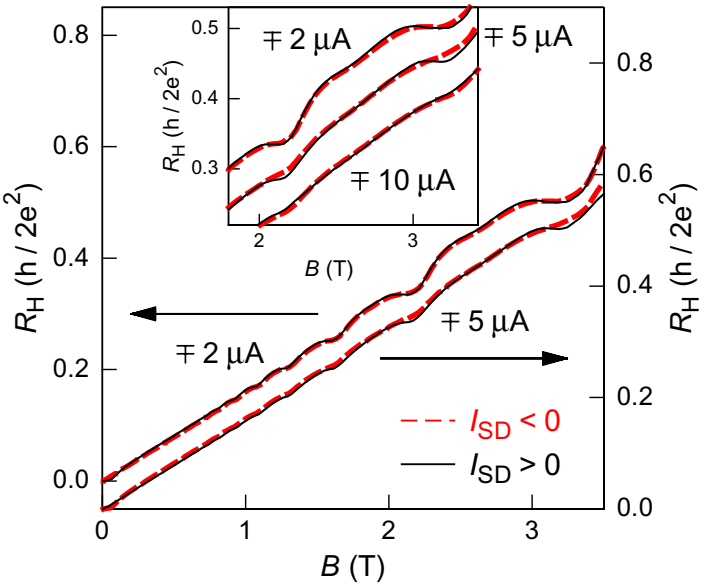

Figure 3. Hall resistance of a Hall bar with a width of $d = 10\,\mu$m defined in wafer I ($\mu \simeq 1.4 \times 10^6\,\mathrm{cm^2\,Vs^{-1}}$). An asymmetric confinement potential is created with $V_L = -1.2\,$V and $V_R = -0.3\,$V causing a hard lhs edge and a soft rhs edge of the Hall bar. The main plot shows R_H for $I_{SD} = \mp 2\,\mu$V (lhs y-axis) and $I_{SD} = \mp 5\,\mu$V (rhs y-axis). The inset displays detailed views of the section including filling factors $\nu = 6$ and $\nu = 4$ of the same data and, in addition, for $I_{SD} = \mp 10\,\mu$A. For clarity, the curves for $|I_{SD}| > 2\,\mu$A in the inset are vertically shifted. To avoid any confusion, we note that broken lines depict always $I_{SD} < 0$, regardless of the color code.

decreases as the current is increased. However, as long as there is at least one incompressible strip across the Hall bar, dissipationless current is possible resulting in the plateau value of R_H. In agreement with the screening theory, we assume two incompressible strips, just one on each edge of the Hall bar [13]. On the one hand, the asymmetric confinement causes the incompressible strip on the softer edge to be wider than the one on the harder edge (for figure 3, the lhs edge), as sketched in figure 1(b). On the other hand, a large current generally results in a widening (narrowing) of the incompressible strip at the edge of the higher (lower) electrochemical potential (figures 1(c) and (d)) [14]. For the higher electrochemical potential on the softer edge (figure 1(c)), the result is therefore a very narrow incompressible strip on the hard edge and a very wide incompressible strip on the soft edge. The direct consequence is a more stable incompressible strip (on the soft edge) and a wider Hall plateau at the onset of the breakdown regime. For the data shown in figure 3, this situation is reached for $I_{SD} > 0$. For the opposite current direction $I_{SD} < 0$, the narrow incompressible strip imposed by the hard edge potential is compensated for by the widening due to the large excess current; however, the wide incompressible strip on the soft edge is reduced in width. Accordingly, the breakdown is already observed for lower absolute values of the current (figure 1(d)).

Within this scenario, it is possible to compensate for a reversal of the lateral asymmetry of the confinement potential by reversing the direction of the impressed current. This prediction [14] is experimentally tested in figure 4, where we plot $R_H(B)$ taken at $I_{SD} = \mp 6\,\mu$m

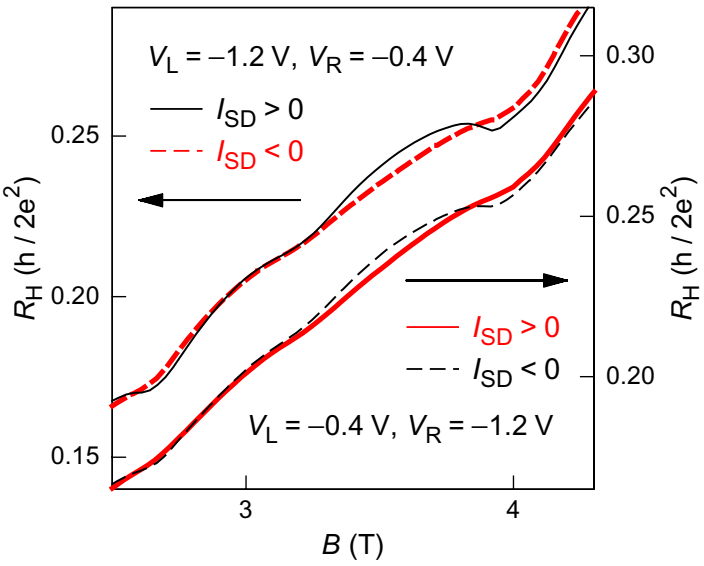

Figure 4. Hall resistance of the same Hall bar as for figure 3 ($d = 10\,\mu$m, $\mu \simeq 1.4 \times 10^6\,\mathrm{cm^2\,Vs^{-1}}$) for $I_{SD} = \mp 6\,\mu$m. In addition to the current direction, the lateral asymmetry is modified exchanging the soft and hard edges. These data were measured after illumination of the sample at $T = 1.7$ K, causing a higher charge carrier density but no qualitative change in the investigated effects.

on the same wafer as above. Between the two sets of curves the asymmetry of the confinement potential is reversed by exchanging the soft and hard edges of the Hall bar (while the magnetic field direction is unchanged). For the harder edge on the lhs of the Hall bar (lhs axis, two curves on top), the Hall effect is more stable for $I_{SD} > 0$, as already observed in figure 3. In contrast, if the lhs edge is the softer one, the Hall effect is more stable for $I_{SD} < 0$. As expected, the general behavior remains unchanged whenever we inverse both, the direction of the current and the direction of the lateral confinement potential. However, a reversal of only one of the two quantities near the onset of the breakdown of the IQHE causes a drastic change in the width of the Hall plateaus. We interpret this behavior as a rectification of the IQHE.

Figure 5 plots an example of the same behavior, but observed on wafer III with a much higher mobility of $\mu \simeq 8 \times 10^6\,\mathrm{cm^2\,Vs^{-1}}$ and a Hall bar width of $d = 3\,\mu$m measured at $I_{SD} = \mp 1\,\mu$A. Here, we apply $V_L = -0.4$ V and $V_R = -1.5$ V defining the harder edge on the rhs of the Hall bar. Note that the smaller absolute value of the breakdown current observed in the high-mobility sample might be explained by a smaller width of this Hall bar. As expected the breakdown of the IQHE is more pronounced for positive current, causing a higher chemical potential at the lhs edge of the Hall bar. In figure 5, we additionally display the longitudinal resistance (rhs y-axis). It shows the breakdown behavior in agreement with the $R_H(B)$ data.

We observe the same behavior over a wide range of mobilities, charge carrier densities, Hall bar widths and contact combinations. While here we show only a small selection of our data, we have performed many control measurements, always leading to the same systematic result, namely rectification of the IQHE in a Hall bar with an asymmetric lateral confinement potential as a function of the direction of the impressed current (at the onset of the breakdown of the IQHE).

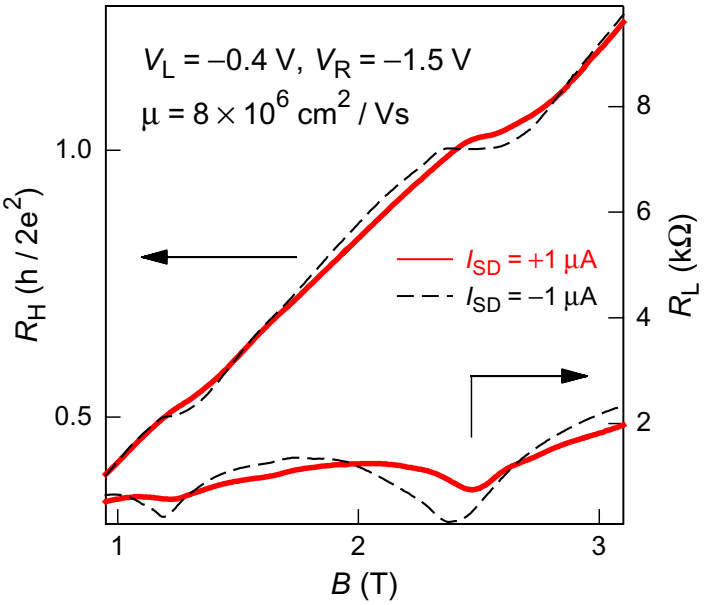

Figure 5. Hall resistance R_H of an asymmetric Hall bar with a width of $d = 3\ \mu$m on wafer III ($\mu \simeq 8 \times 10^6\,\mathrm{cm^2\,Vs^{-1}}$) for $I_{SD} = \mp 1\ \mu$m. Also shown are the corresponding longitudinal resistances R_L (rhs y-axis).

In the following, we discuss our results in light of conventional theories versus the screening theory of the IQHE. Both the original bulk and edge theories fail to describe the experimentally observed smooth transition regions between the plateaus of the Hall resistance (and the corresponding finite longitudinal resistance) in a self-contained way. Instead the transition between Hall plateaus is phenomenologically explained by assuming broadening of the Landau levels and corresponding narrowing of the Hall plateaus. Hence, one would expect a narrowing of the Hall plateaus as the mobility is decreased (and the disorder is increased). However, in experiments the opposite behavior is observed, namely the plateaus become wider as the mobility is decreased. To heal this discrepancy, the localization is—again phenomenologically—invoked, such that disorder induces localized states, which then results in broader plateaus for the low-mobility samples and causes an insulating bulk state. The edge theories take, in addition, the confinement potential into account, as the edge states are a direct result of the Landau levels cutting the Fermi energy at the edges of the Hall bar. However, no detailed assumptions are made regarding the shape of the confinement potential.

In our experiments, we observe the effect of an impressed current on the Hall resistance (altering the transition regions between the plateaus) as a function of the lateral shape of the confinement potential. In this regime, we cannot expect the conventional theories to explain our findings. Moreover, calculations within these conventional models are performed in the linear response regime, whereas here we use large currents, clearly putting us out of the linear response regime.

The screening theory is based on numerical calculations of the exact shape of the confinement potential by taking the direct Coulomb interaction between charge carriers as well as their quantum mechanical properties into account [13, 14]. In contrast to the conventional theories, the screening theory allows self-consistent numerical calculations even in the nonlinear

response regime, which results in predictions at the onset of the breakdown regime of the IQHE. The observed rectification of the IQHE at the onset of its breakdown is beyond the scope of conventional theories. Our results qualitatively confirm the predictions of the screening theory. It should be noted that the present form of the screening theory does not account for the local temperature (and local heating effects) in a self-consistent way. However, a reasonable prescription for such a calculation is already given in the literature [30]. In this calculation scheme, a large impressed current melts (narrows) the incompressible strips, finally leading to the experimentally observed breakdown. While the screening theory predicts the width and location of incompressible strips omitting local heating effects, the additional assumption of local heating as treated in [30] results in qualitative agreement with our experiments.

4. Summary

In summary, we have experimentally investigated the current-induced breakdown of the IQHE on narrow, gate-defined and high-mobility Hall bars. As a function of a lateral confinement potential, where one edge of the Hall bar is hard and the other is soft, we find an asymmetric breakdown of the IQHE. In detail, the hard edge tends to become highly dissipative for a large current, while the dissipation-suppressed edge channel stays stable along the soft edge. The observations cannot be explained within the conventional theories of the IQHE, but are in agreement with the predictions of the emerging screening theory.

Acknowledgments

AS thanks D Harbusch and D Taubert for their technical support and J P Kotthaus for trusting a theorist performing experiments in his institute. Financial support from the German Science Foundation via SFB 631, the Germany–Israel program DIP and the German Excellence Initiative via the 'Nanosystems Initiative Munich (NIM)' is acknowledged. AS is partially supported by IU-BAP:6970.

References

[1] Klitzing K V, Dorda G and Pepper M 1980 New method for high-accuracy determination of the fine-structure constant based on quantized Hall resistance *Phys. Rev. Lett.* **45** 494
[2] Das Sarma S and Pinczuk A 1997 *Perspectives in Quantum Hall Effects* (New York: Wiley)
[3] Ahlswede E, Weitz P, Weis J, von Klitzing K and Eberl K 2001 Hall potential profiles in the quantum Hall regime measured by a scanning force microscope *Physica* B **298** 562
[4] Ilani S, Martin J, Teitelbaum E, Smet J H, Mahalu D, Umansky V and Yacoby A 2004 *Nature* **427** 328
[5] Horas J, Siddiki A, Moser J, Wegscheider W and Ludwig S 2008 Investigations on unconventional aspects in the quantum Hall regime of narrow gate defined channels *Physica* E **40** 1130–2
[6] Siddiki A, Horas J, Moser J, Wegscheider W and Ludwig S 2009 Interaction-mediated asymmetries of the quantized Hall effect *Europhys. Lett.* **88** 17007
[7] Laughlin R B 1981 *Phys. Rev.* B **23** 5632
[8] Halperin B I 1982 *Phys. Rev.* B **25** 2185
[9] Büttiker M 1986 Four-terminal phase-coherent conductance *Phys. Rev. Lett.* **57** 1761
[10] Chklovskii D B, Shklovskii B I and Glazman L I 1992 Electrostatics of edge states *Phys. Rev.* B **46** 4026
[11] Kramer B, Kettemann S and Ohtsuki T 2003 Localization in the quantum Hall regime *Physica* E **20** 172

[12] Lier K and Gerhardts R R 1994 Self-consistent calculation of edge channels in laterally confined two-dimensional electron systems *Phys. Rev.* B **50** 7757
[13] Siddiki A and Gerhardts R R 2004 Incompressible strips in dissipative Hall bars as origin of quantized hall plateaus *Phys. Rev.* B **70** 195335
[14] Siddiki A 2009 Current-directioninduced rectification effect on (integer) quantized Hall plateaus *Eur. Phys. Lett.* **87** 17008–14
[15] Güven K and Gerhardts R R 2003 Self-consistent local-equilibrium model for density profile and distribution of dissipative currents in a Hall bar under strong magnetic fields *Phys. Rev.* B **67** 115327
[16] Siddiki A, Eksi D, Cicek E, Mese A I, Aktas S and Hakioğlu T 2008 Theoretical investigation of the electron velocity in quantum Hall bars, in the out of linear response regime *Physica* E **40** 1217–9
[17] Dempsey J, Gelfand B Y and Halperin B I 1993 Electron–electron interactions and spontaneous spin polarization in quantum Hall edge states *Phys. Rev. Lett.* **70** 3639–42
[18] Ihnatsenka S and Zozoulenko I V 2006 Spatial spin polarization and suppression of compressible edge channels in the integer quantum Hall regime *Phys. Rev.* B **73** 155314
[19] Siddiki A 2008 The spin–split incompressible edge states within empirical Hartree approximation at intermediately large Hall samples *Physica* E **40** 1124–6
[20] Bilgeç G, Üstünel Toffoli H, Siddiki A and Sokmen I 2010 The self-consistent calculation of exchange enhanced odd integer quantized Hall plateaus within Thomas–Fermi–Dirac approximation *Physica* E **42** 1058–61
[21] Eber G, von Klitzing K, Ploog K and Weinmann G 1983 Two-dimensional magneto-quantum transport on GaAs–$Al_xGa_{1-x}As$ heterostructures under non-ohmic conditions *J. Phys. C: Solid State Phys.* **16** 5441–8
[22] Kirtley J R, Schlesinger Z, Theis T N, Milliken F P, Wright S L and Palmateer A L 1986 Low-voltage breakdown of the quantum Hall state in a laterally constricted two-dimensional electron gas *Phys. Rev.* B **34** 1384–7
[23] Komiyama S, Kawaguchi Y, Osada T and Shiraki Y 1996 Evidence of nonlocal breakdown of the integer quantum Hall effect *Phys. Rev. Lett.* **77** 558–61
[24] Cage M E, Dziuba R F, Field B F, Williams E R, Girvin S M, Gossard A C, Tsui D C and Wagner R J 1983 Dissipation and dynamic nonlinear behavior in the quantum Hall regime *Phys. Rev. Lett.* **51** 1374–7
[25] Molenkamp L W, Brugmans M J P, van Houten H, Beenakker C W J and Foxon C T 1991 Voltage-probe-controlled breakdown of the quantum Hall effect *Phys. Rev.* B **43** 12118–21
[26] Oto K, Sanuki T, Takaoka S, Murase K and Gamo K 2002 Two types of breakdown of quantum Hall effect depending on the electron density fluctuation *Physica* E **12** 173–7
[27] Güven K, Gerhardts R R, Kaya I I, Sagol B E and Nachtwei G 2002 Two-level model for the generation and relaxation of hot electrons near the breakdown of the quantum Hall effect *Phys. Rev.* B **65** 155316
[28] Sağol B E, Nachtwei G, von Klitzing K, Hein G and Eberl K 2002 Time scale of the excitation of electrons at the breakdown of the quantum Hall effect *Phys. Rev.* B **66** 075305
[29] Arslan S, Cicek E, Eksi D, Aktas S, Weichselbaum A and Siddiki A 2008 Modeling of quantum point contacts in high magnetic fields and with current bias outside the linear response regime *Phys. Rev.* B **78** 125423
[30] Kanamaru S, Suzuuara H and Akera H 2006 Spatial distributions of electron temperature in quantum Hall systems with compressible and incompressible strips *J. Phys. Soc. Japan* **75** 064701